27/28th International Conference
ENGINEERING MECHANICS 2022
Milovy, Czech Republic, May 9 –12, 2022
Paper **#88,** pp. 153–156, doi: 10.21495/51-2-153

AEROELASTIC INSTABILITY OF DIFFERENTLY POROUS U-PROFILES IN CROSSWIND DIRECTION

Hračov S.[*], Macháček M.[**]

Abstract: *Flow-induced vibrations of the flexibly mounted slender U-shaped beams allowed to oscillate in the crosswind direction only are studied experimentally in the wind tunnel. All beams are characterized by a cross section having a side ratio of along-wind to across-wind dimension equal to two. The effects of two depths of U profiles and two porosities of their flanges (0 % and 75 %) onto a loss of aeroelastic stability are investigated under the smooth flow conditions and for low Scruton numbers. The results indicate almost similar proneness of the non-porous beams to galloping-type oscillations to a rectangular prism with the same side ratio regardless their depth. The onset of across-wind galloping occurred in these cases at wind velocity very close to von-Kármán-vortex-resonance flow speed, even though the critical velocity predicted by the quasi-steady theory is much lower. For porous and shallower U profile this asynchronous quenching also takes place. However, the higher flange porosity reduces significantly not only the vortex-shedding effect, but also causes an increase in the onset galloping velocity above the critical speed determined for non-porous profiles. In the case of deeper U-shaped beam, the effect of higher porosity even suppresses the proneness to galloping.*

Keywords: Aeroelastic instability, Galloping, Vortex shedding, Asynchronous quenching, U profile.

1. Introduction

The study of aeroelastic instability of long slender bluff bodies in the crosswind direction has been of great interest in the field of civil engineering during last decades (Holmes, 2014). The prediction of a potential occurrence of unnecessary or even damage oscillations of, e.g., transmission lines, antenna shafts and cylindrical parts of telecommunication towers or bridge pylons and cables during a design stage is crucial for their subsequent safe operation without any serious serviceability problems. Two main phenomena related to undesirable oscillation of an isolated structure normal to the wind flow are usually distinguished. The first represents the vortex-induced vibration (Blevins, 2001), the latter galloping (Paidoussis, 2014). Both are characterized by nearly harmonic oscillation at frequency close to natural frequency of the system. Vortex-induced vibration (VIV) should be checked according to standard (EN 1991-1-4, 2010) for bodies with ratio of the largest to the smallest crosswind dimension of the structure, both taken in the plane perpendicular to the wind, higher than 6. The maximum of the response caused by vortex shedding effect is reached at the critical wind velocity, V_{VIV}, when the frequency of vortex-shedding is the same as a natural frequency of the structure, f_{VL}. The vortex-shedding frequency is proportional to the Strouhal number, S_T, and actual wind speed, V, and inversely proportional to the width of structure, D. Thus, for critical wind velocity V_{VIV} it holds:

$$V_{VIV} = D \cdot f_{VL}/S_T \tag{1}$$

The galloping instability occurs unlike VIV only for non-circular cross sections. The onset wind velocity for galloping, V_{CG}, is proportional to the Scruton number, S_C, to the natural frequency of the structure, f_{VL}, and to the width of structure and is inversely proportional to factor of instability, a_G:

$$V_{CG} = 2S_C \cdot D \cdot f_{VL}/a_G \tag{2}$$

This stability factor corresponds to the slope of the transversal force coefficient obtained from measurements of aerodynamic forces in the wind tunnel. In case of closeness of theoretically determined

---

[*] Ing. Stanislav Hračov, Ph.D.: Institute of Theoretical and Applied Mechanics AS CR, Prosecká 76, 19000, Prague, CZ, hracov@itam.cas.cz

[**] Ing. Michael Macháček, Ph.D.: Institute of Theoretical and Applied Mechanics AS CR, Prosecká 76, 19000, Prague, CZ, machacek@itam.cas.cz

critical wind velocities for vortex-shedding and galloping the interaction of both phenomena can occur. European standard (EN 1991-1-4, 2010) recommends to consult the possibility of so-called quenching effect with specialist, if the ratio of critical velocity for galloping and vortex shedding is in the range from 0.7 to 1.5.

In this paper, the aeroelastic stability of U-shaped beams in the across wind direction is experimentally investigated in the wind tunnel. All tested beams have U - shaped cross section corresponding to side ratio SR = 2. This profile is expected to be susceptible to galloping according to previous aerodynamic measurements (Hračov, 2020). The influence of depth and porosity of both flanges of the U profile onto the general proneness and onset velocity of galloping is studied. The results are also compared with the outputs from identical wind tunnel testing of the rectangular prisms with three different side ratios.

2. Experimental setup

All experimentally tested U-shaped specimens have the same basic geometry *(L x B x D - 100 x 20 x 10 cm)* and were made from plywood rectangular cylinders and plastic flanges with specific degree of fill. In total, four beams, which differ in the depth of their cross section, $D_B = 1/2\ D$ and $D_B = 2/3\ D$, or in the flange porosity, $p = 0\%$ and $p = 75\%$, were fabricated and analyzed, see Figure 1. In addition, the rectangular prisms with the same length, L, and width, B, as the U beams and with three different heights, D_R, were tested. The non-porous U beams is expected to gallop similarly to the rectangular cylinder with the largest height corresponding to $SR = 2$. On the other hand, the rectangular prisms with $SR = 4$ and 6 represent the limiting cases to almost fully porous U profiles with $D_B = 1/2\ D$ and $D_B = 2/3\ D$, respectively. The mechanical properties of the analyzed specimens measured at still-air conditions are stated in Table 1. In this table also the Strouhal number, S_T, the instability parameter, a_G, and angular interval of positive slope of transversal coefficient, $\langle \alpha\text{-};\ \alpha+ \rangle$, that were determined from previous aerodynamic measurements (Hračov, 2020) of identical profiles, are given. Based on these parameters, the reduced vortex-shedding-resonance wind velocity, $V_{VIV} / f_{VL} D$, and reduced onset galloping wind velocity, $V_{CG} / f_{VL} D$, were calculated, see Table 1. The examples of the power spectral density of lift force measured by the authors on static shallower U beams and on the rectangular prism with $SR = 2$ from which V_{VIV} and S_T were determined are depicted in Figure 2.

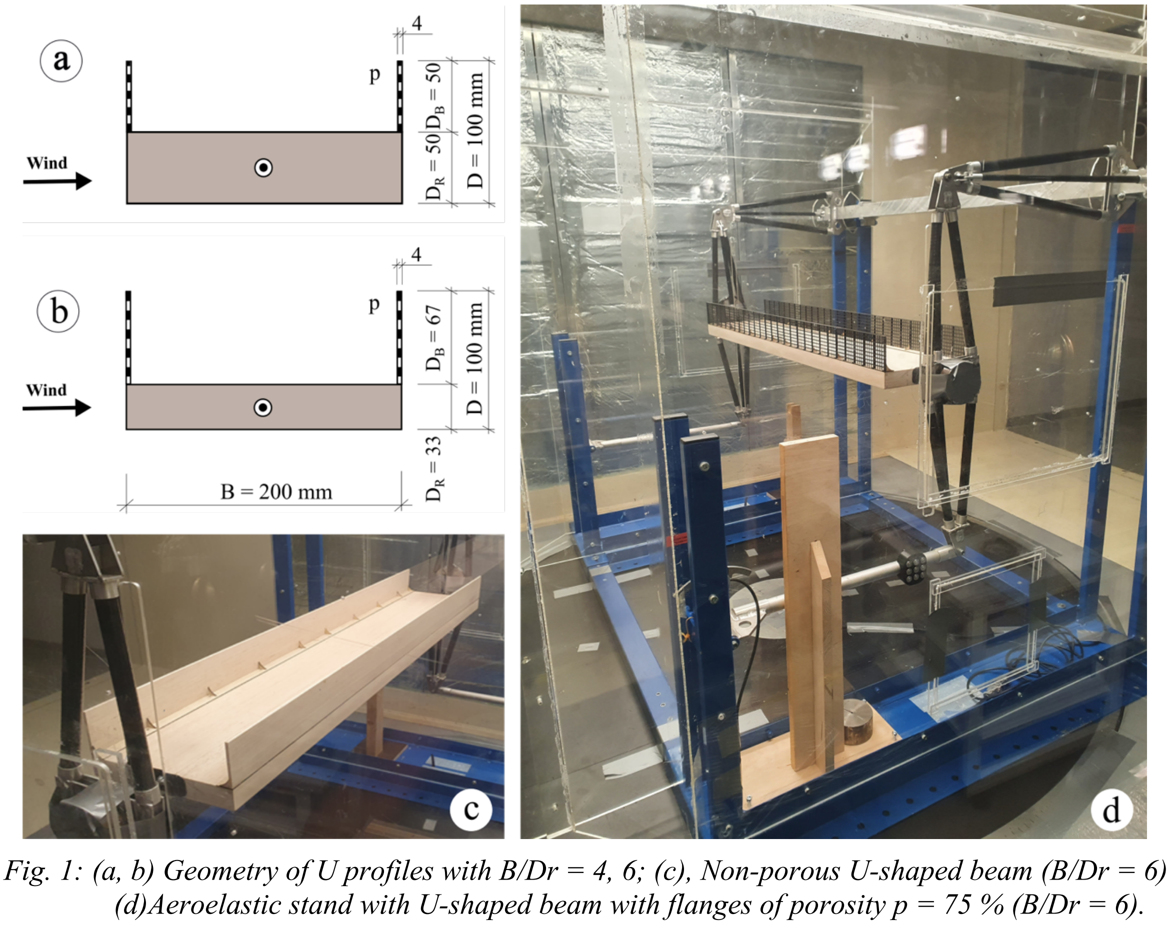

Fig. 1: (a, b) Geometry of U profiles with B/Dr = 4, 6; (c), Non-porous U-shaped beam (B/Dr = 6) (d)Aeroelastic stand with U-shaped beam with flanges of porosity p = 75 % (B/Dr = 6).

All specimens were fixed horizontally in a specially designed stand located in the aerodynamic section of the wind tunnel of ÚTAM AV ČR in Telč in the Czech Republic, see Fig. 1. This stand allows to restrict a movement of the models only in the across wind direction and to tune their natural frequencies to almost identical value. The plexiglass end plates were installed at both ends of the models to reduce the boundary effect. All tests were performed under practically smooth flow conditions. The testing of each specimen started from wind speed, V, approx. equal to 2 m/s. The wind velocity was then increased step-by-step by small value ΔV=0.5 m/s. For each step, i.e., each velocity, a steady-state transversal response was measured using the rotary transducer. The data from the sensor were recorded for 60 s with a sampling frequency fs = 1000 Hz. The increase in wind velocity was stopped after the excessive vibrations occurred or if there was a danger of static failure of the model. Subsequently, the wind velocity was gradually decreased and the steady - state response was measured at several wind speeds in order to detect the presence of possible hysteretic effect.

Tab. 1: Structural properties of aeroelastic models and predicted reduced critical wind speeds.

Cross section	B/D_R [/]	p [%]	m [g]	f_{VL} [Hz]	ζ [%]	S_C [/]	S_T [/]	$\langle\alpha_-; \alpha_+\rangle$ [/]	a_G [/]	$\frac{V_{VIV}}{f_{vl} D}$ [/]	$\frac{V_{CG}}{f_{vl} D}$ [/]	$\frac{V_{CR}}{f_{vl} D}$ [/]
Rectangle	2	-	1953	4.78	0.40	8.7	0.086	⟨-6.2; 6.2⟩	9.8	11.7	1.8	11.4
Rectangle	4	-	1900	4.97	0.50	42.3	0.142	-	-	7,0	-	-
Rectangle	6	-	1872	4.91	0.55	103	-	-	-	-	-	-
U-profile	4	0	1981	4.78	0.48	10.6	0.090	⟨-8.7; 5.3⟩	7.48	11.1	2.8	11.6
U-profile	4	75	2017	4.76	0.51	11.4	0.067	⟨-4.1; 2.5⟩	7.56	14.9	3.0	17.3
U-profile	6	0	1969	4.75	0.58	12.7	0.089	⟨-8.2; 5.6⟩	8.15	11.3	3.1	11.3
U-profile	6	75	2001	4.77	0.54	12.0	-	⟨-4.0; 0.6⟩	2.31	-	10.4	-

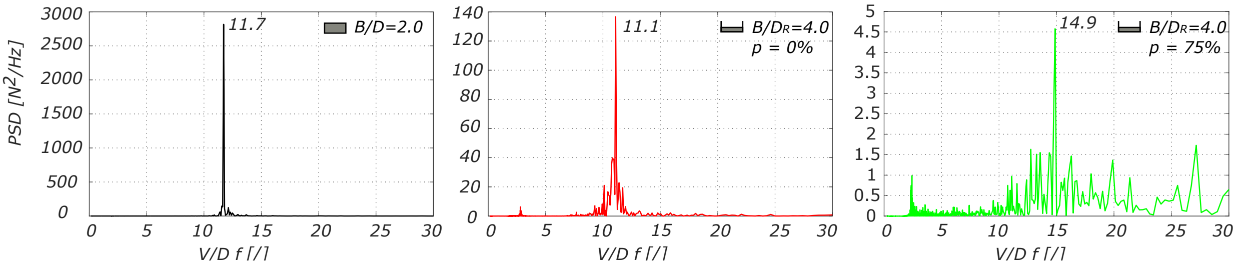

Fig. 2: Power spectral density of the across wind force as a function of normalized frequency for a rectangular profile with B/D = 2 and non-porous and porous U-shaped profiles with B/Dr = 4

3. Results and discussion

The graphs in Figure 3 present the standard deviation of the transversal displacement of all tested models normalized to the height, D, and measured for various wind speeds. The solid lines correspond to the part of the test with a gradual increase in the wind speed, while the dashed curves with square symbols to the part, when the wind speed was decreasing. The circular marks on solid lines indicate the reduced wind speeds, $V_{CR} / f_{VL} D$, for which a harmonic character of the response was first observed. These velocities are given in the far right column of Table 1.

Left graph in Figure 3 shows the comparison of responses for prisms with rectangular cross-sections with $SR = 2$ and 4 and for both shallower U beams with $D_b = 1/2\ D$. The unrestricted galloping-type oscillations of rectangular prism with $SR = 2$ and non-porous U beam occurs around the reduced velocity equal to 11.4 and 11.6 respectively. These velocities are significantly higher than the critical galloping wind speeds determined by the quasi-steady theory, but they are very close to the vortex-shedding resonance wind speeds, see Table 1. It implies that there exists the so-called quenching effect. An interaction between the VIV and galloping leads to suppression of the latter one until the wind speed, for which the vortex-shedding frequency match the natural frequency, is reached.

For porous U profile with D_b =*1/2 D*, a shift of galloping onset towards the higher wind velocities in comparison with non-porous case is noticeable. It can be caused by a rather broadband character of vortex-shedding with spectrum peaks located at higher reduced velocities, while for the non-porous profile a dominant peak of spectrum is present, see Figure 2. The higher and lower amplitudes of limit cycle oscillation than for rectangle with SR = 2 were determined for non-porous and porous U profile, respectively. It corresponds well with the angular intervals of the positive slope of the transversal force coefficient for each individual case in Table 1. As expected, no self-limited response was determined for the rectangle with *SR = 4*.

The dotted lines in Figure 3a correspond to steady-state response determined at low reduced speeds after an initial displacement of about 10 mm was imposed to the models. While for the rectangular prism with *SR = 4* it represents the classical vortex-induced vibration, for other profiles the secondary mode of vortex-shedding caused by the resonance with impinging leading-edge vortices was excited. In the cases of aeroelastic models in Figure 3b, the dotted lines are missing since their behavior after initial displacement was not analyzed.

The response recorded for the non-porous U beam with higher depth, D_b =*2/3 D*, follows the response of the rectangular prism with *SR = 2*, see Figure 3b. The origin of the galloping-type oscillations occurs similarly to the non-porous shallower U-profile at the reduced vortex-shedding critical velocity. The combination of larger depth and high porosity substantially affects the susceptibility of U-shaped beam to a loss of across-wind stability. No sign of galloping or vortex-induced vibration was present even for very high-reduced velocities. This holds also for the rectangular prism with *SR = 6*, which is in good agreement with the predictions of the quasi-steady theory.

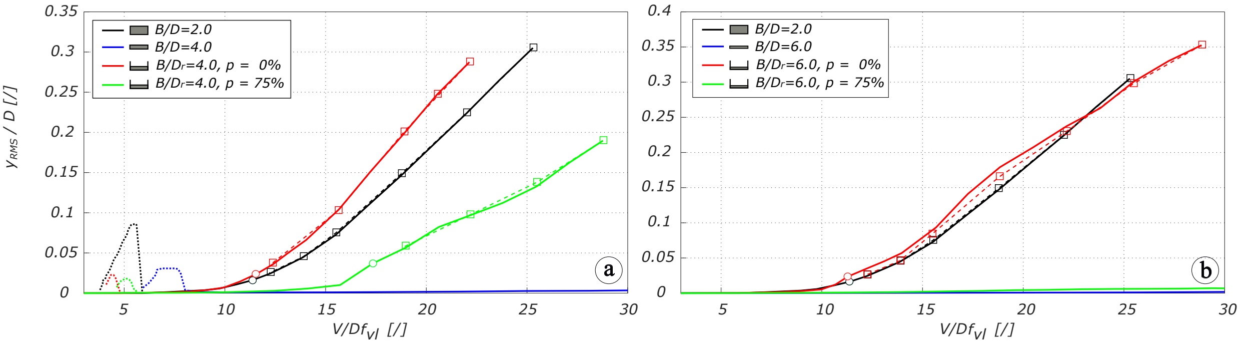

Fig. 3: Normalized across-wind response (RMS value) as a function of reduced wind speed
(a) rectangular profiles with side ratios B/D = 2, 4 and U-shaped profiles with B/Dr = 4
(b) rectangular profiles with side ratios B/D = 2, 6 and U-shaped profiles with B/Dr = 6

The experimental campaign highlighted the possibility of the presence of the quenching effect in the cases of U-shaped beams with *SR = 2*. The interaction of vortex-shedding and galloping was identified for ratios of critical wind velocities related to these phenomena even outside the range defined by standard (EN 1991-1-4, 2010). The quasi-steady theory failed to predict the onset galloping velocity; however, it provides the information about a general proneness to this type of aeroelastic instability. In addition to that, no significant hysteretic behavior was observed for any of the measured rectangular and U-shaped beams.

Acknowledgement

The kind support of Czech Scientific Foundation project No. 19-21817S and RVO 68378297 institutional support are gratefully acknowledged.

References

Blevins, R.D. (2001). *Flow-Induced Vibration*, Krieger Pub Co, Malabar, Florida, USA.

EN 1991-1-4 (2010). Eurocode 1 – Actions on structures – Part 1-4: General actions – Wind actions. CEN/TC 250, Brussels, Belgium.

Holmes, J.D. (2015). *Wind Loading of Structures*, CRC Press, Taylor & Francis Ltd, London, UK.

Hračov, S., Macháček, M., (2021), Aerodynamic wind tunnel testing of U-beams, *Computational Mechanics 2021*, Srní, Czech Republic, pp. 621-630.

Paidoussis, M.P., Price, S.J., de Langre, E. (2014). *Fluid-structure Interactions: cross-flow induced instabilities*, Cambridge University Press, New York, NY, USA.